Aust. J. Phys., 1979, **32**, 155–72

A Comparison of Effective Two-nucleon Interactions Appropriate for Use in Analyses of Inelastic Nucleon Scattering*

R. Smith[A] *and K. Amos*[B]

[A] Department of Theoretical Physics, Research School of Physical Sciences, Australian National University, P.O. Box 4, Canberra, A.C.T. 2600.
[B] School of Physics, University of Melbourne, Parkville, Vic. 3052.

Abstract

A comparison of the spatial and fourier components of a number of effective two-nucleon interactions, suitable for use in analyses of inelastic nucleon scattering data, is complemented by a comparison of their use in a variety of distorted wave analyses. Specifically, a set of effective interactions derived from 'realistic' potentials have been compared, not only with each other, but also with a semi-phenomenological valence interaction that has been developed over recent years and has been used extensively in reaction data analyses.

1. Introduction

A prime objective of analyses of direct reaction scattering from nuclei is to ascertain what details are valid for any model spectroscopy that is applicable to the nuclei involved. Analyses of nucleon inelastic scattering data in particular afford useful tests of microscopic models of nuclear structure, not only because a variety of data can be obtained in these experiments, including spin-dependent data such as analysing powers, but also because such reactions reflect the single-particle transition densities of the spectroscopy and are therefore complementary as tests of that spectroscopy to the predictions of electromagnetic transition rates. Indeed recent studies (Amos *et al.* 1978; Kennedy *et al.* 1978) have demonstrated that proton inelastic scattering is particularly sensitive to neutron excitations in the target and therefore can be more instructive than the $B(\mathrm{E}L)$ predictions of the same spectroscopy.

To take advantage of the stringent test of spectroscopy that is offered by analyses of inelastic nucleon scattering, it is essential that all significant components of the reaction mechanism be known and that an appropriate representation of each such attribute of the reaction mechanism be specified. A number of data analyses, particularly those for transitions involving excitations of unnatural parity states, have established the important components of the direct interaction mechanism (Love and Satchler 1971; Geramb *et al.* 1975, and references cited therein; Bertsch *et al.* 1977; Smith *et al.* 1978). These studies have shown that an effective two-nucleon (valence) interaction comprising at least central and tensor force parts, and possibly also a two-body spin–orbit force term, is required in analyses of all data in the direct reaction energy range ($\sim$10–200 MeV nucleons). Additionally, for most natural parity transitions, and since microscopic models of spectroscopy

* Research supported by a grant from the Australian Research Grants Committee.

of the electromagnetic properties of such transitions invariably require polarization charges to match observed data, core polarization corrections must be included in inelastic scattering data analyses. By analogy with the electromagnetic transition corrections, inelastic scattering core polarization corrections have been represented usually by a collective model prescription of the form factors involved (Love and Satchler 1971; Nesci and Amos 1977). In fact the correlation between effective charges and core polarization corrections to inelastic scattering transition amplitudes has been useful in predicting $B(EL)$ values. The connection between the two is broken, however, if the transition spectroscopy is dominated by neutron excitations (Amos *et al.* 1978; Kennedy *et al.* 1978). Thus transition data whose analyses require little core polarization correction are required in order to test with least uncertainty the character of the valence contributions.

It may also be necessary to account for other reaction mechanism components in analyses and these must be treated appropriately, or conditions selected specifically to minimize their roles, in order that inelastic scattering data may be used most effectively to test various valence interactions. Of all such components one may contemplate, two seem most likely. The first involves formation of virtual particles (a deutron in particular). However, while there have been claims of significant effects from this component, our studies (Geramb *et al.* 1975; Nesci and Amos 1977; Rikus *et al.* 1977; Smith *et al.* 1978) have revealed little need to include such effects in (p, p′) analyses, but some need, although by no means a major one, in (p, n) data analyses. Indeed far more important than these higher order corrections are those in which giant resonances of the target act as doorway states (Geramb *et al.* 1975) in processes by which the projectile is captured and a nucleon, bound initially in the target, is ejected. These resonance processes are all quite energy dependent so that by selecting 'non-collective' data taken with sufficiently high projectile energy (>30 MeV for heavy nuclei) only the valence interaction components in transition amplitudes should be important.

Of all the important reaction processes (for inelastic nucleon scattering) noted above, only the valence interaction component yields transition amplitudes free from any of the uncertainties implicit in the use of collective model representations and their attendant form factors. Thus, for any circumstances under which only valence interaction contributions are important, transition data give the most significant test of details of the chosen microscopic model of spectroscopy. Conversely, given transitions for which microscopic models of spectroscopy are well established (little or no core polarization correction required) and for conditions that make virtual particle and resonance effects insignificant (sufficiently high projectile energies, for example) then transition data can be used to test the characteristics of any appropriate valence interaction. Such was the case in recent work by Bertsch *et al.* (1977) and Borysowicz *et al.* (1977), although their choice of reaction data for analysis was more for illustrative purposes than for use as a critical assessment of the various effective interactions that they derived from an assortment of realistic two-nucleon potentials.

It is the purpose of the present study to use inelastic scattering data as a more critical test of these various effective valence interactions and to compare their general characteristics, as well as their specific effects in inelastic scattering analyses, with those of a standard (and perhaps simpler) semi-phenomenological effective interaction that has been used with considerable success in a number of previous

analyses of inelastic scattering data (Geramb *et al.* 1975; Nesci and Amos 1977; Amos *et al.* 1978; Kennedy *et al.* 1978; Smith *et al.* 1978, and references cited therein).

Details of the various effective valence interactions are given in the next section while the specifics of the reaction analyses are presented in Section 3. Finally the results of these analyses are discussed in Section 4.

2. Effective Interactions

All the effective interactions considered herein can be expanded generally in the form

$$t(01) = \sum_{ST} V_{\text{cen}}^{ST}(01)\, P^S P^T + \sum_{T} V_{\text{ten}}^{1T}(01)\, S_{01}\, P^T + \sum_{T} V_{\text{so}}^{1T}(01)\, \boldsymbol{L}.\boldsymbol{S} P^T, \tag{1}$$

where the quantities V_{cen}, V_{ten} and V_{so} are functional forms of the (local) central, tensor and two-body spin–orbit forces respectively. The superscripts S (T) assume values 0 or 1 according to the projection operators P selecting singlet or triplet spin (isospin) two-body channels, and we identify the operators by expectation values, whence for

$$S_{01} = 3(\boldsymbol{\sigma}_0.\boldsymbol{r})(\boldsymbol{\sigma}_1.\boldsymbol{r})/r^2 - (\boldsymbol{\sigma}_0.\boldsymbol{\sigma}_1) \tag{2}$$

we have

$$\langle {}^3S_1 | S_{01} | {}^3D_1 \rangle = \sqrt{8}, \tag{3}$$

whilst for

$$\boldsymbol{L}.\boldsymbol{S} = (\boldsymbol{r}\times\boldsymbol{p}).(\boldsymbol{\sigma}_0+\boldsymbol{\sigma}_1)/2\hbar \tag{4}$$

we have

$$\langle {}^3P_0 | \boldsymbol{L}.\boldsymbol{S} | {}^3P_0 \rangle = -2. \tag{5}$$

In these equations $\boldsymbol{r}$ is the relative coordinate vector and the states in the expectation values are two-particle spin–angle functions:

$$|{}^{(2S+1)}L_J\rangle = \sum_{M_L M_S} \langle L S M_L M_S | J M_J \rangle\, Y_{LM_L}(\Omega_{01}) | \tfrac{1}{2}\tfrac{1}{2} S M_S \rangle. \tag{6}$$

A variety of forms are considered herein for the radial functions in equation (1); specifically those used in a number of inelastic scattering analyses (e.g. Geramb *et al.* 1975; Smith *et al.* 1978) and those derived from fitting G-matrix elements of 'realistic' forces (e.g. Borysowicz *et al.* 1977).* These sets of effective interactions are listed in Table 1, together with the strengths of various components in each two-body channel. This table classifies the effective interaction by a prefix (the first letter of which indicates the nature of the force and the next two letters give the two-body spin–isospin channel in which it acts) followed in parentheses by an abbreviation for the authors of the original effective interaction or realistic potential. Thus, for example, CSE (WW) denotes the central singlet–even potential of the effective interaction due to Wong and Wong (1967). The symbolism is fully detailed in the footnote to Table 1.

* The effective interactions of Borysowicz *et al.* (1977) differ from their subsequently published results (Bertsch *et al.* 1977) in that the latter set uses only three Yukawa ranges compared with the four ranges used by Borysowicz *et al.* In the present paper we have chosen to make comparisons with the effective interactions of Borysowicz *et al.* The slightly simpler (fewer ranges) Bertsch *et al.* set produces an almost identical variation in coordinate space and in the low momentum fourier transforms.

Table 1. Classification and strengths of effective interactions

No.	Classification Name[A]	*ST*	Type	Strengths (MeV) V_1	V_2	V_3	V_4
Standard interaction							
1	CSE(WW)	01	Central	−25·0			
2	CTE(WW)	10	Central	−47·0			
3	TTE(EH)	10	Tensor	−105·25	−1·9481		
4	TTO(EH)	11	Tensor	17·918	−2·3085	0·3831	
5	STE(EH)	10	Spin–orbit	−213·91			
6	STO(EH)	11	Spin–orbit	−282·41	−5·1793		
RD interaction							
7	CSE(RD)	01	Central	−5294·5	−3007·8	2419·2	
8	CTE(RD)	10	Central	−12040·9	−2776·3	3012·9	
9	TTE(RD)	10	Tensor	28717·7	−537·0	421·4	28·3
10	STO(RD)	11	Spin–orbit	30001·5	−10·6	−1·2	
HJ interaction							
11	CSE(HJ)	01	Central	−493·3	−2716·1	1754·3	10·463
12	CTE(HJ)	10	Central	−11418·0	1131·1	597·0	10·463
13	TTE(HJ)	10	Tensor	−981·6	−947·8	800·95	
EL interaction							
14	TTO(EL)	11	Tensor	−3884·4	245·6	−210·5	
15	STE(EL)	10	Spin–orbit	2033·4	643·4	−103·8	
16	STO(EL)	11	Spin–orbit	26803·7	195·6	−38·9	

[A] The first letter of the name indicates the nature of the force (C, central; T, tensor; S, spin–orbit), the next two letters give the two-body spin–isospin channel (S, singlet; T, triplet; E, even; O, odd) and the abbreviation in parentheses gives the origin of the effective interaction (WW, Wong and Wong 1967; EH, Eikemeier and Hackenbroich 1971; RD, Reid 1968; HJ, Hamada and Johnston 1962; EL, Elliott *et al.* 1968).

The radial functions in the effective interactions of Table 1 have the form

$$V(r) = \sum_i V_i f(r/R_i) \tag{7}$$

for the central and spin–orbit components and

$$V(r) = \sum_i V_i r^2 f(r/R_i) \tag{8}$$

for the tensor force part. The precise nature of these forms and the ranges involved are given in Table 2.

The effective interaction defined hereafter as the Standard interaction (Wong and Wong 1967; Eikemeier and Hackenbroich 1971) involves a mixture of gaussian functions and is composed of terms 1–6 in Tables 1 and 2. This form has been used extensively, and with considerable success, in a variety of inelastic nucleon scattering analyses and will be compared here with interactions derived from fitting a sum of Yukawa forms to the *G*-matrix elements of the 'realistic' interactions due to Reid (1968; terms 7–10 in Tables 1 and 2) and Hamada and Johnston (1962; terms 11–13). Neither of these effective interactions, to be referred to henceforth as RD

Table 2. Character and ranges of radial functional forms in effective interactions
The functions $f(r/R_i)$ of equations (7) and (8) are specified

No.	Character Name	Form	Range (fm) R_1	R_2	R_3	R_4
Standard interaction						
1	CSE(WW)	Gaussian	1·907			
2	CTE(WW)	Gaussian	1·721			
3	TTE(EH)	Gaussian	0·960	2·034		
4	TTO(EH)	Gaussian	1·146	1·383	2·234	
5	STE(EH)	Gaussian	0·747			
6	STO(EH)	Gaussian	0·756	1·021		
RD interaction						
7	CSE(RD)	Yukawa	0·2	0·4	0·5	
8	CTE(RD)	Yukawa	0·2	0·4	0·5	
9	TTE(RD)	Yukawa	0·2	0·4	0·5	0·7
10	STO(RD)	Yukawa	0·2	0·4	0·5	
HJ interaction						
11	CSE(HJ)	Yukawa	0·2	0·4	0·5	1·414
12	CTE(HJ)	Yukawa	0·2	0·4	0·5	1·414
13	TTE(HJ)	Yukawa	0·2	0·4	0·5	
EL interaction						
14	TTO(EL)	Yukawa	0·2	0·4	0·5	
15	STE(EL)	Yukawa	0·2	0·4	0·5	
16	STO(EL)	Yukawa	0·2	0·4	0·5	

and HJ respectively, has a contribution in the triplet–odd tensor (TTO) channel and so both forms have been supplemented by the addition of that component from the interaction (EL) due to Elliott *et al.* (1968; term 14).

At this point a comment should be made concerning the absence of central odd-state potentials from Tables 1 and 2. It has often been observed that, whilst direct and exchange distorted wave amplitudes are constructive for the even-state parts of the central force, those for the odd states are destructive (Love and Satchler 1970; Satchler 1973). In fact the calculations of Bertsch *et al.* (1977) using central odd-state potentials derived from the EL interaction indicated that the inclusion of odd-state components had typically only a 2% or 3% effect on cross-section predictions for inelastic nucleon scattering. Since most data are accurate to only 5% it is not surprising that the effective interactions in common use, including that we have referred to as the Standard interaction, have seen no need to include such components. Indeed, heavy ion analyses, which may be sensitive only to the direct terms, may offer the only means of investigating such components.

We have then three prescriptions for the effective interactions to be used in inelastic nucleon scattering analyses, with the one recommended by Borysowicz *et al.* (1977) being that we have classified as RD. In Fig. 1 therefore we compare the configuration space variations (labelled by R) and fourier transforms (labelled by K) of the RD interaction (dashed curves) with those of the Standard interaction (solid curves). It is evident that the general trends are the same although the short-range properties of the RD interaction are quite different in the central components, with a sign

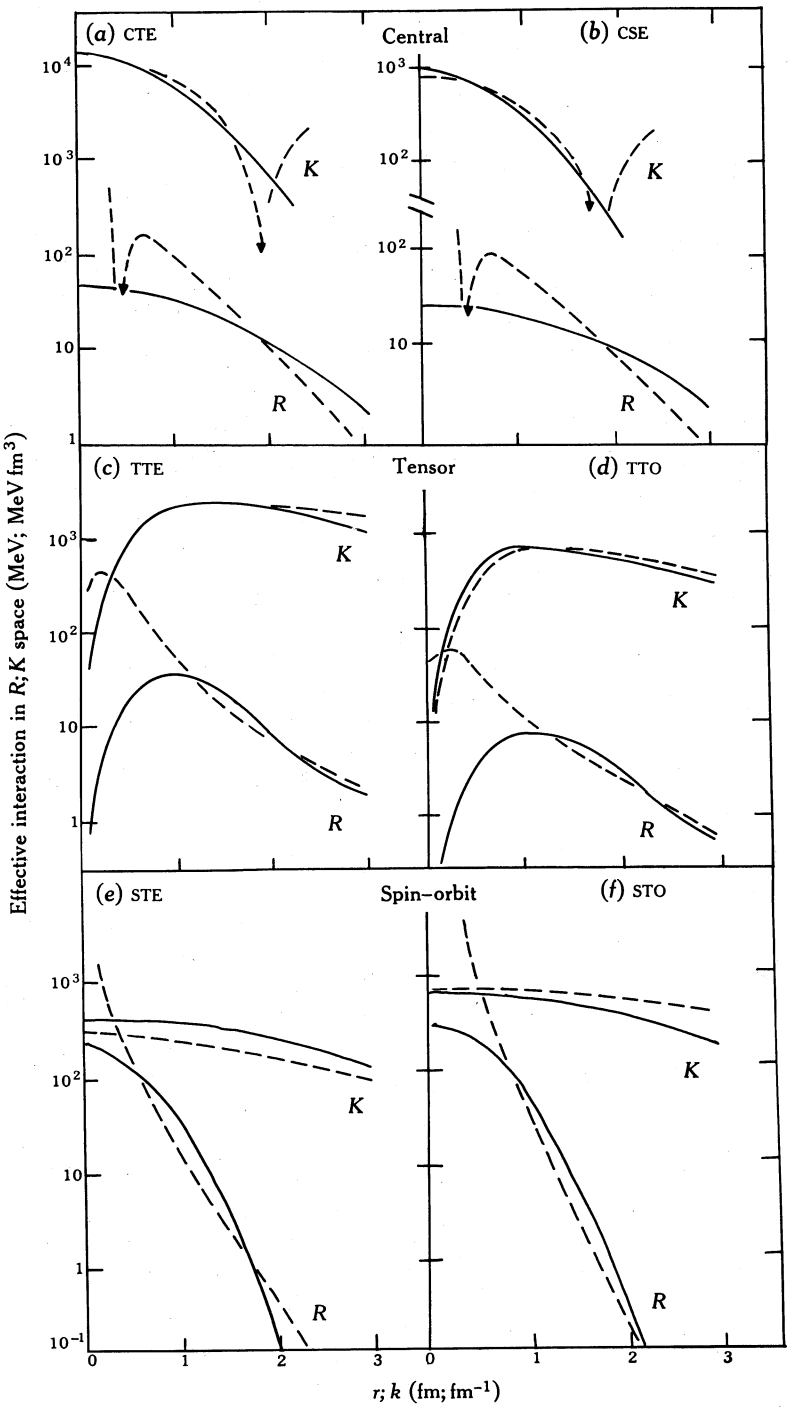

Fig. 1. Comparison of the properties in coordinate space R and momentum space K of the Standard effective interaction (solid curves) with those of the RD effective interaction (dashed curves). The effective interactions and components are as defined in Table 1. The RD triplet–odd tensor force used is the TTO (EL) component in Table 1 and the triplet–even spin–orbit force is STE (EL). The arrows shown on four of the RD interaction curves indicate a decreasing value that changes sign at smaller arguments.

change occurring (i.e. a long-range attraction and a short-range repulsion). The short-range repulsion dominates such forces for large momentum components ($k > 2\,\mathrm{fm}^{-1}$) where it produces a relatively large repulsive tail in momentum space, in sharp contrast to the uniformly attractive tail of the Standard interaction form. The importance of such high momentum components in distorted wave calculations is by no means understood and these differences should be borne in mind in the comparison of the different central force distorted wave predictions to follow. It is apparent, however, that the fourier transforms for all other terms, and for the central terms for components in momentum space $<2\,\mathrm{fm}^{-1}$, compare very closely.

Table 3. Multipole moment integrals of effective interactions

All values for the J_L integrals are in units of MeV fm^{2+L}. The values in parentheses are obtained using the alternative effective interaction expansion of Bertsch *et al.* (1977)

Name	J_0	J_2	J_4
CSE (WW)	−965	−5265	−47867
CSE (RD)	−849 (−1011)	−3250(−6503)	−20967 (−186600)
CSE (HJ)	−893 (−868)	−6484(−5929)	−192259(−184300)
CTE (WW)	−1335	−5932	−43944
CTE (RD)	−1290(−1530)	−4665(−8009)	−28403 (−192700)
CTE (HJ)	−1072(−1068)	−6464(−6343)	−187920(−185900)
TTE (EH)	−1281	−7502	−90097
TTE (RD)	−1630(−1333)	−7707(−6640)	−116471(−93515)
TTE (HJ)	−1132(−1234)	−7075(−8943)	−83310 (−162900)
TTO (EH)	376	2726	40118
TTO (EL)	400 (391)	1948(2390)	22087 (39500)
STE (EH)	−496	−416	−580
STE (EL)	−559 (−654)	−301 (−628)	−406 (−2009)
STO (EH)	−710	−630	−957
STO (RD)	−3005(−1077)	−713 (−605)	−539 (−1399)
STO (EL)	−2790(−1023)	−706 (−675)	−542 (−1778)

An alternative, and perhaps more significant, measure of the effects of any force in reaction analyses is given by the low multipole moments, defined by

$$J_L = 4\pi \int_0^\infty r^{L+2}\, V(r)\, \mathrm{d}r, \tag{9}$$

where the $V(r)$ are the radial parts of the forces obtained by omitting the operators S_{01} and $\boldsymbol{L}.\boldsymbol{S}$ in equation (1). The J_L results for the effective interactions considered here are given in Table 3. The corresponding J_0 and J_2 values of all force components for the different models are very similar and the structural differences of the forces begin to show up significantly only in the J_4 values, which highlight the configuration space differences at distances greater than 2 fm.

As a final comparison, which has also been used in previous analyses (Bertsch *et al.* 1977; Borysowicz *et al.* 1977), we consider the oscillator matrix elements of the effective interactions. Borysowicz *et al.* compared 10 harmonic oscillator matrix elements calculated from the separated HJ potential with the matrix elements

calculated from their Yukawa fit. To these values we have appended the expectations from our Standard interaction, and the results are given in Table 4, from which a generally good agreement is immediately apparent (typically 5–10 % disparity).

In summary then, significant differences between the effective interactions derived from realistic potentials and the extensively used semi-phenomenological effective interaction are seen only in the high momentum components and high (J_4) moments of the interactions. It remains to be seen if such differences can be distinguished in distorted wave analyses of inelastic nucleon scattering data.

Table 4. Comparison of S-wave oscillator matrix elements for single-even components

The results are obtained using an oscillator energy of 14 MeV

n	n'	Matrix elements calculated from: separated HJ potential[A]	Yukawa fit[A]	Standard interaction
0	0	−5·61	−5·69	−5·86
1	0	−4·70	−4·72	−4·46
1	1	−4·53	−4·55	−4·22
2	0	−3·61	−3·60	−3·08
2	1	−3·72	−3·76	−3·51
2	2	−3·34	−3·40	−3·37
3	0	−2·62	−2·61	−2·06
3	1	−2·84	−2·89	−2·75
3	2	−2·71	−2·76	−2·97
3	3	−2·38	−2·45	−2·88

[A] Values as tabulated previously by Bertsch *et al.* (1977) and Borysowicz *et al.* (1977).

3. Distorted Wave Analyses

In the microscopic distorted wave approximation (DWA) the measurables associated with direct reaction nucleon scattering from nuclei are all related to transition amplitudes of the form (Geramb and Amos 1971)

$$\begin{aligned} T_{\mathrm{fi}} &= A\langle\chi_{\mathrm{f}}^{(-)}(0)\,\psi_{J_{\mathrm{f}}M_{\mathrm{f}}}(1,\ldots,A)\,|\,t(01)\,|\,\mathscr{A}_{01}\{\chi_{\mathrm{i}}^{(+)}(0)\,\psi_{J_{\mathrm{i}}M_{\mathrm{i}}}(1,\ldots,A)\}\rangle \\ &= \sum_{j_1 j_2 I} S(j_1,j_2;J_{\mathrm{i}},J_{\mathrm{f}};I)\,\mathscr{M}(j_1,j_2;J_{\mathrm{i}},J_{\mathrm{f}};I), \end{aligned} \tag{10}$$

where the spectroscopic amplitudes are defined by the reduced matrix element

$$S(j_1,j_2;J_{\mathrm{i}},J_{\mathrm{f}};I) = \langle\psi_{J_{\mathrm{f}}}\|[a_{j_2}^{\dagger}\times a_{j_1}]^{I}\|\psi_{J_{\mathrm{i}}}\rangle \tag{11}$$

and the two-particle amplitudes are

$$\begin{aligned} \mathscr{M} = \sum_{m_1 m_2 N} (-)^{j_1-m_1}&\langle j_1,j_2,m_1,-m_2\,|\,I-N\rangle(2J_{\mathrm{f}}+1)^{-\frac{1}{2}} \\ &\times\langle J_{\mathrm{i}},I,M_{\mathrm{i}},N\,|\,J_{\mathrm{f}},M_{\mathrm{f}}\rangle\langle\chi_{\mathrm{f}}^{(-)}(0)\,\phi_{j_2m_2}(1)\,|\,t(01)\,|\,\mathscr{A}_{01}\{\chi_{\mathrm{i}}^{(+)}(0)\,\phi_{j_1m_1}(1)\}\rangle. \end{aligned} \tag{12}$$

Here the $\chi^{(\pm)}$ are the distorted waves, the single-nucleon bound states ϕ_{jm} are obtained

by cofactor expansions of the many-particle nuclear states $|\psi_{JM}\rangle$, and $\mathscr{A}_{01}$ is the two-particle antisymmetrization operator.

All details of the derivation of the above equations, of the notation and of their evaluation when the effective interaction $t(01)$ takes the central, tensor and spin–orbit operator forms of equations (1)–(5) are given in earlier publications (Geramb and Amos 1971; Geramb *et al.* 1975; Smith 1976). We wish to draw one selection rule from these publications, however. The radial forms of the effective interaction of equation (1), expressed generally in two-nucleon spin and isospin channels by

$$t(01) = \sum_{ST} A_{ST}(r_{01})\, P^S P^T, \tag{13}$$

can be expanded in multipoles, whence

$$A_{ST}(r_{01}) = \sum_{LM} 4\pi A^L_{ST}(r_0, r_1)\, Y_{LM}(\Omega_0)\, Y^*_{LM}(\Omega_1). \tag{14}$$

The standard vector coupling techniques for the direct matrix elements then identify the interaction multipole L for the central component with the orbital angular momentum transfer quantum number. Thus L is constrained by the following relationships between angular momentum transfer and parity:

$$\boldsymbol{I} = \boldsymbol{J}_\mathrm{i} - \boldsymbol{J}_\mathrm{f}, \qquad S = 0, 1, \tag{15a}$$

$$\boldsymbol{I} = \boldsymbol{L} + \boldsymbol{S}, \qquad \pi_\mathrm{i}\pi_\mathrm{f} = (-)^L. \tag{15b}$$

The multipole selection rules for the tensor and two-body spin–orbit operators are more complex, however, with the direct amplitudes for each being determined by a number of multipoles with values equal to or near the total angular momentum transfer quantum number. No such identifications exist for the exchange amplitudes which can receive contributions from all multipoles of the interaction but, to the extent that the data prediction is sensitive to the direct amplitudes, a judicious choice of the reaction will allow the selective investigation of specific multipoles of the interaction.

The multipole selection facility discussed above together with the two reaction constraints discussed in the Introduction (namely reliable available spectroscopy to reduce or eliminate the core polarization amplitude, and data taken for transitions with sufficient energy that competing reaction mechanisms are not significant) have guided the selection of the four sets of data, detailed below, for analysis as a reliable basis to compare the interactions of Tables 1 and 2.

Inelastic proton scattering to the first and second excited states of ^{89}Y will allow us to investigate the triplet two-body isospin components of the effective interactions, as both excitations are well described by single-proton transitions. The ground state of ^{89}Y is considered to be a $2p_{1/2}$ proton plus an ^{88}Sr core and the states studied are the $9/2^+$ state at 0·908 MeV and the $3/2^-$ state at 1·5 MeV. A zero-order shell model description assumes for the $9/2^+$ state a $1g_{9/2}$ proton outside an ^{88}Sr core whilst the $3/2^-$ state is considered to be a $2p_{3/2}$ hole plus an additional proton in the already half-filled $2p_{1/2}$ subshell. This description of the $9/2^+$ state (Morrison *et al.* 1977) has been used extensively in previous inelastic scattering analyses (Geramb

and Amos 1971; Geramb 1972) and has required only minor core polarization corrections, in agreement with the prediction of the model that the $9/2^+$ state should decay to the ground state via an M4–E5 γ-ray with a transition rate of 5–6 s, compared with the experimental γ-ray transition rate of 13–16 s. The description of the $3/2^-$ state is certainly poorer and will consequently require a significant core polarization correction to describe the transition, but it does represent the dominant part of the wavefunction (Vergados and Kuo 1971).

Specifically therefore, the scattering of 24·5 MeV protons to the $3/2^-$ (1·5 MeV) state of ^{89}Y has been analysed as a test of the low multipoles ($L = 0, 2$ for the central direct component). The single-particle bound states were described by a Woods–Saxon well which has been deemed appropriate in previous work (Geramb 1972), with the continuum particle optical model parameters and data being taken from the work of Benenson *et al.* (1968).

Table 5. Spectroscopic factors used in reaction analyses

The spectroscopic factors are as defined in equation (11). Proton and neutron bound states are indicated by π and ν respectively

Target	J_i^π	J_f^π	j_1	j_2	I	$S(j_1,j_2;J_i,J_f;I)$
^{89}Y	$1/2^-$	$3/2^-$	$2p_{3/2}(\pi)$	$2p_{1/2}(\pi)$	1	1·7321
					2	−2·2361
^{89}Y	$1/2^-$	$9/2^+$	$2p_{1/2}(\pi)$	$1g_{9/2}(\pi)$	4	3·0
					5	3·3166
^{90}Zr	0^+	0^+(IAS[A])	$2p_{1/2}(\nu)$	$2p_{1/2}(\pi)$	0	0·2475
			$1g_{9/2}(\nu)$	$1g_{9/2}(\pi)$	0	0·8877
^{28}Si	0^+	$6^-(T=0)$	$1d_{5/2}(\pi)$	$1f_{7/2}(\pi)$	6	1·7388
			$1d_{5/2}(\nu)$	$1f_{7/2}(\nu)$	6	1·7388
^{28}Si	0^+	$6^-(T=1)$	$1d_{5/2}(\pi)$	$1f_{7/2}(\pi)$	6	1·7388
			$1d_{5/2}(\nu)$	$1f_{7/2}(\nu)$	6	−1·7388

[A] Isobaric analogue of the ground state.

The higher multipoles ($L = 3, 5$) have been examined using the scattering of 61·4 MeV protons to the $9/2^+$ state of ^{89}Y, the data being those of Scott *et al.* (1969), the optical model parameters being taken from the work of Fulmer *et al.* (1969) and the bound states being described by a harmonic oscillator well of strength 9·18 MeV.

The single-proton transition descriptions used above limit the usefulness of reaction analyses to an investigation of only the triplet isospin two-body components. In order to study the singlet isospin channels therefore we have also analysed (p, n) data to the isobaric analogue of the ground state of ^{90}Zr and (p, p′) data to the high spin (6^-; $T = 0, 1$) unnatural parity states in ^{28}Si, both of which involve significant neutron excitations in the full spectroscopic descriptions.

Specifically, direct reaction (p, n) data initiated by 35 MeV protons (Doering *et al.* 1975) to the isobaric analogue of the ground state of ^{90}Zr will be sensitive to the $L = 0$ central multipole. The ground state of ^{90}Zr is well described by two (valence) protons weakly coupled to an ^{88}Sr core constrained to the $2p_{1/2}$–$1g_{9/2}$ 'shell' and the final state in the reaction, namely the 0^+ state in ^{90}Nb, is taken as the isobaric analogue, the details of this description and the resultant spectroscopic

factors being given in a previous paper (Rikus *et al.* 1977). For simplicity and because all relevant elastic scattering data have not been obtained, all optical model potential parameters were derived from the Bechetti and Greenlees (1969) prescription, and the bound states are represented by harmonic oscillator wavefunctions evaluated using an oscillator energy of 9·16 MeV.

The higher multipoles ($L = 5$ for central direct) have been investigated using the inelastic scattering of 135 MeV protons (Adams *et al.* 1977) to two 6^- states in ^{28}Si ($T = 0$, 11·6 MeV; $T = 1$, 14·4 MeV). A transition spectroscopy of $(1d_{5/2})^{-1}(1f_{7/2})$ particle–hole excitations from a projected Hartree–Fock intrinsic ground state is used (Smith *et al.* 1978) with the bound states generated in a 13·5 MeV harmonic oscillator well and the optical model taken from fits to the elastic scattering of 155 and 100 MeV protons from ^{28}Si for the entrance and exit channels respectively (Willis *et al.* 1968; Horowitz 1972).

For completeness, the spectroscopic factors derived from the nuclear state descriptions detailed above and the optical model parameters used in all analyses are listed in Tables 5 and 6 respectively.

Table 6. Optical model parameters

Target nucleus	E_{lab} (MeV)	V_0 (MeV)	r_0 (fm)	a_0 (fm)	W_0 (MeV)	$4W_D$ (MeV)	r_D (fm)	a_D (fm)	V_{so} (MeV)	r_{so} (fm)	a_{so} (fm)	r_c (fm)
^{89}Y	24·5	46·57	1·232	0·627	0	43·68	1·275	0·627	0	—	—	1·31
^{89}Y	61·4	39·5	1·2	0·69	5·12	10·16	1·403	0·53	6·59	1·027	0·83	1·25
^{90}Zr	35·0	49·04	1·17	0·75	5·0	17·53	1·32	0·51	6·2	1·01	0·75	1·25
	22·97	46·97	1·17	0·75	3·52	24·63	1·26	0·58	6·2	1·01	0·75	—
^{28}Si	135	22·7	1·29	0·7	11·0	0	1·26	0·67	2·78	0·95	0·62	1·25
	Exit[A]	21·7	1·27	0·68	6·18	0	1·55	0·42	9·54	1·08	0·61	1·29

[A] $T = 0$ and 1 states at 11·6 and 14·4 MeV respectively.

4. Results

The results of our reaction analyses are presented in Figs 2–5 below, where in each case we compare the predictions of the Standard, RD and HJ effective interactions for each of the central and tensor components separately and for the total (central plus tensor) prediction. In all figures the Standard interaction prediction is depicted by the solid curve, the RD prediction by the dashed curve and the HJ prediction by the dot–dash curve. Also shown separately is the prediction of the TTO(EL) tensor component (dotted curve) which is common to both the RD and HJ effective interaction prescriptions.

No attempt has been made here to further investigate the two-body spin–orbit components beyond the comparisons made in Section 2. Those comparisons indicated that the RD and HJ forms are very similar in configuration and momentum space to the Standard form and, as the Standard form has been found to make only negligible contribution in previous analyses of the reactions under examination here (Rikus *et al.* 1977; Smith *et al.* 1978), we have not pursued the spin–orbit comparisons further. One exception to this is the analysis of transitions to high spin states, for example, the ^{28}Si 6^- states (Smith *et al.* 1978), where the Standard spin–orbit form produced non-negligible results but gave incorrect relative magnitude predictions for the isovector and isoscalar transitions, a result which led us to infer that the role of an $\boldsymbol{L}.\boldsymbol{S}$ force should be small. Indeed the only way to delineate the role of a

two-body $\boldsymbol{L}.\boldsymbol{S}$ component may be to analyse the spin-dependent measurables (asymmetry, polarization and spin-flip probability) for transitions for which reliable spectroscopy is available (Lebrun *et al.* 1976).

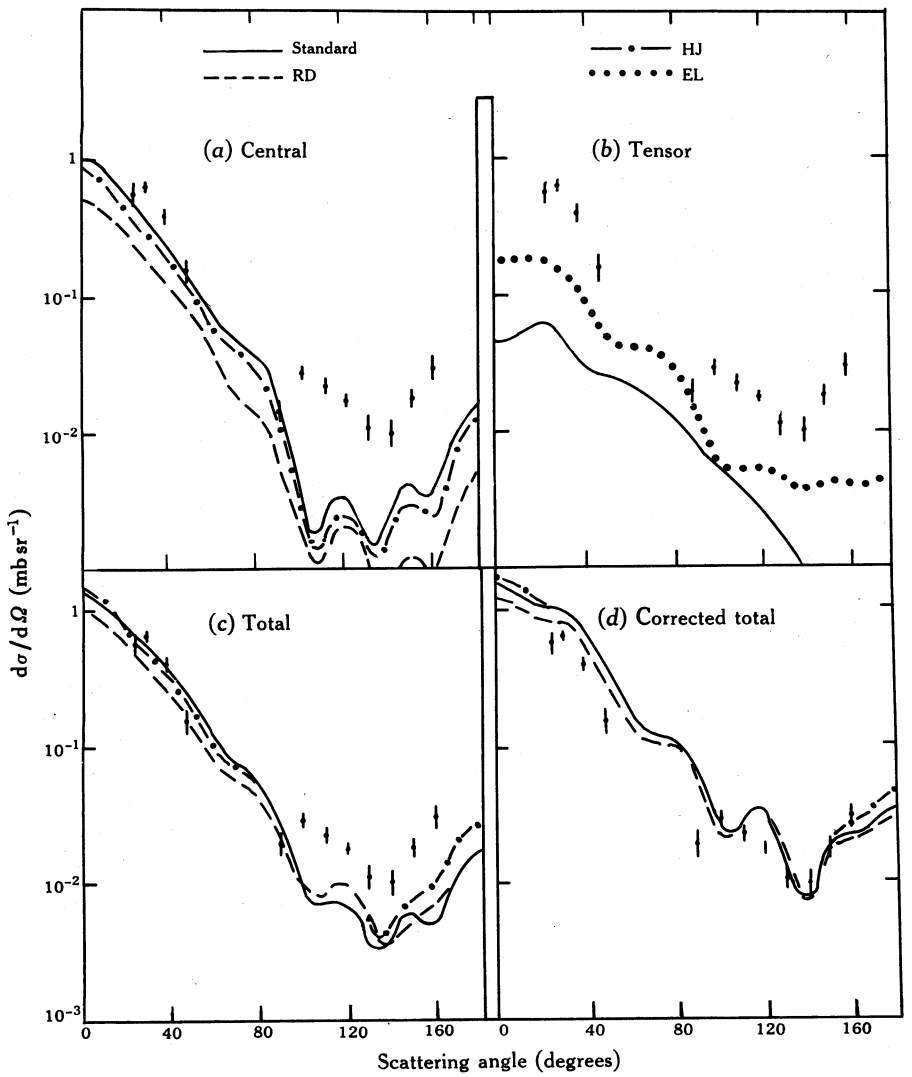

Fig. 2. Comparison between the Standard, RD and HJ effective interaction results for the differential cross section from DWA analyses of the inelastic scattering of 24·5 MeV protons leading to the $3/2^-$ (1·5 MeV) state in ^{89}Y. In (*b*) the RD and HJ results found by using only their tensor force components are identical (only the triplet–odd channel) and are of the EL interaction form. The total (central plus tensor) cross section predictions in (*c*) are supplemented by a small core polarization correction to give the satisfactory fit to the experimental data shown in (*d*).

The analyses of the excitation of the $3/2^-$ (1·5 MeV) state in ^{89}Y by 24·5 MeV protons are shown in Fig. 2. This excitation, which is described by a single-proton transition and hence is sensitive only to the $T = 1$ two-body components of the effective interactions, and is selective of the low multipoles of the interaction ($L = 0, 2$ for the central direct component), is dominated by the central components for which

it is seen that all three effective interaction prescriptions predict essentially identical cross section structure. The Standard and HJ forms predict comparable magnitudes also and exceed the RD predictions by a factor of approximately 1·5 at forward angles. It should be noted that we also compared the HJ central prediction shown in Fig. 2 with the DWA cross section prediction using an alternative effective interaction, also derived from the long-range part of the Hamada–Johnston potential (Love *et al.* 1969). The DWA cross section prediction obtained using

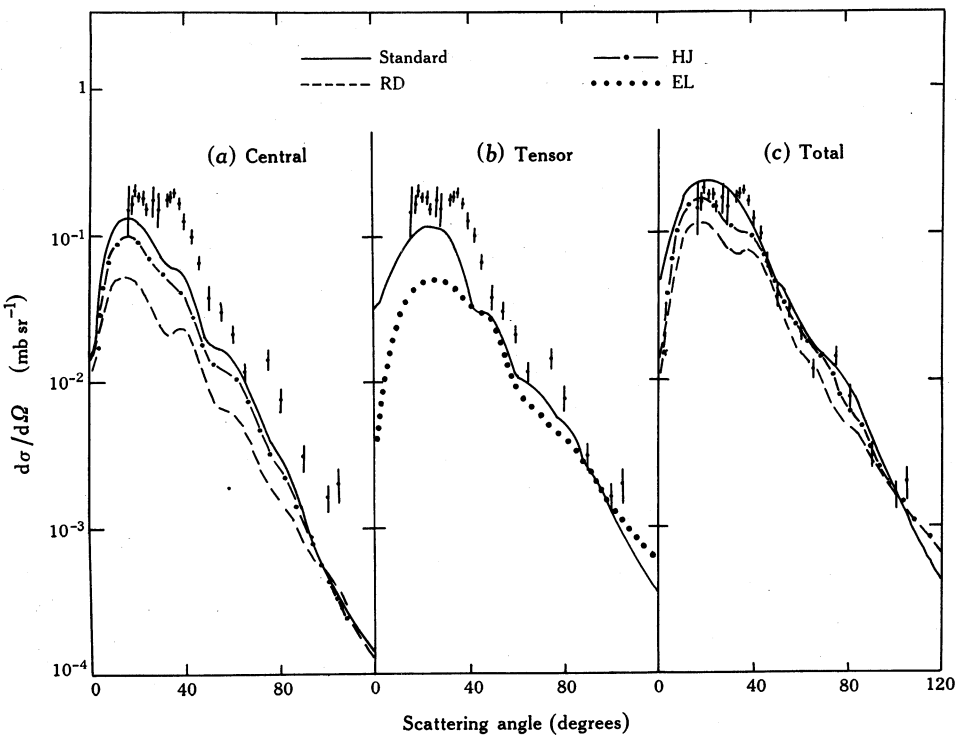

Fig. 3. Comparison of central, tensor and total force effective interaction results from DWA analyses of the inelastic scattering of 61·4 MeV protons exciting the $9/2^+$ (0·908 MeV) state in ^{89}Y.

this alternative Hamada–Johnston form was found to be almost identical with that shown as the HJ central result in Fig. 2. The tensor components act only in the triplet–odd channel and, while they are significantly less than the central prediction and hence have only a minor influence on the total cross section, it is clear that the low multipoles of the TTO(EL) form have a quite different character from the Standard TO term. Specifically the TTO(EL) cross section prediction exceeds that of the Standard interaction by a factor of approximately 2 at forward angles and has different falloff characteristics with angle.

All three effective interactions yield almost identical total cross section predictions and all are in excellent agreement with the experimentally observed structure and magnitude at forward angles. The back angle discrepancies of all interactions are removed if a small core polarization correction is included (Fig. 2*d*); a stiffness parameter C_2 of 600 MeV is appropriate, in agreement with previous analyses using this spectroscopic description (Geramb 1972).

The higher triplet isospin multipoles of the force are examined in Fig. 3 which compares the predictions of the scattering of 61·4 MeV protons to the $9/2^+$ (0·908 MeV) state in ^{89}Y. As for the low multipole comparison, the Standard and HJ central form predictions compare closely and are significantly larger and in better agreement with the data than the RD. Unlike the case for the lower multipoles, however, the Standard tensor form predicts a forward peaked cross section which *exceeds* that of the EL form and has a structure in better agreement with the data.

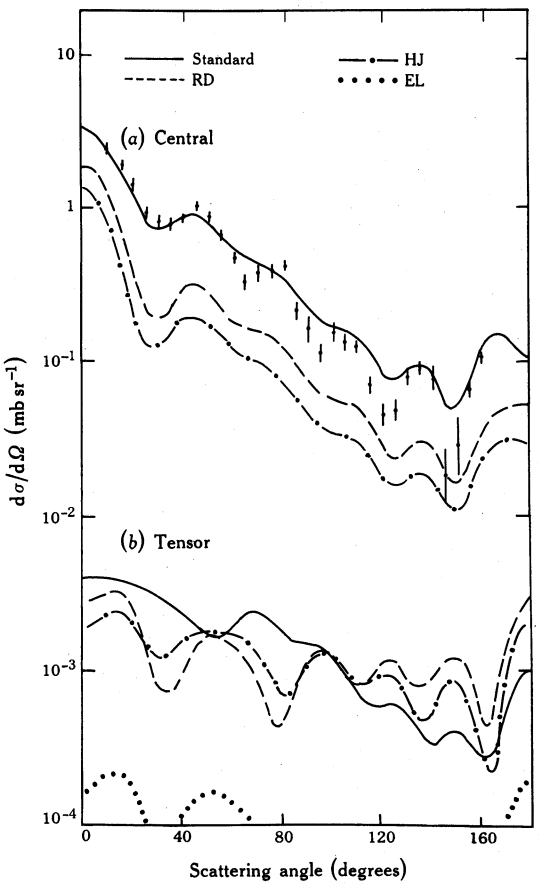

Fig. 4. Comparison of central and tensor force effective interaction results from DWA analyses of the charge exchange scattering of 35 MeV protons exciting the isobaric analogue of the ground state of ^{90}Zr. The central interaction components so dominate in these analyses that the total results are indistinguishable from those shown for the central force, which are compared with the experimental data.

These differences in structure and magnitude are reflected in the total force comparisons, where the tensor component makes a significant contribution and produces a total prediction for the Standard interaction in excellent agreement with the data. The prediction of the total HJ form is acceptable, the small discrepancy at forward angles in part being attributable to the need to add a core polarization correction, albeit small, to all predictions, but the RD form underestimates the magnitude of the

forward angle cross section by a factor of approximately 1·5. All three forms, however, produce results in agreement with the data for scattering angles in excess of 40°.

To this point we have investigated only the two-body triplet isospin interaction components. To extend this to the singlet isospin channels we must analyse transitions promoted by the excitation of bound neutrons. The analysis of the charge exchange scattering of 35 MeV protons exciting the isobaric analogue of the ground state of ^{90}Zr, which is shown in Fig. 4, will be sensitive to the low multipoles of both the $T = 0$ and 1 two-body channels. The tensor force predictions of all three interactions are three orders of magnitude smaller than the data, and in fact the analysis is so dominated by the central component that the total results are indistinguishable from the central and so are not shown separately in Fig. 4.

Unlike the preceding analyses (i.e. those sensitive only to the $T = 1$ channels), the ^{90}Zr(p, n) analysis yields significant differences in the predictions of all three central effective interaction forms. The RD interaction again underestimates the cross section magnitude by a factor of approximately 1·5 but now the HJ form, which has produced results in agreement with the Standard form for the analyses limited to the $T = 1$ channel, underestimates the data by a factor of approximately 2. By comparison the Standard form provides an excellent fit to the data over the full angular range.

The prediction of the Standard force is also seen to be superior to that of the other two forms for the analyses of 135 MeV proton scattering to the 6^- states ($T = 0$, 11·6 MeV; $T = 1$, 14·4 MeV) of ^{28}Si, as shown in Fig. 5. This transition, promoted by both $T = 0$ and 1 high multipole components, is dominated by the tensor terms and all tensor interactions reproduce the bell-shaped angular distribution required by the data and have comparable magnitudes. The central components, on the other hand, predict very different magnitudes for the different interaction forms and distinctly different structures. The Standard central prediction is quite small for transitions to both the $T = 0$ and 1 states and consequently has little effect on the total prediction, but structurally the Standard central form reproduces the experimentally observed cross section. This is certainly not true of the other two forms where, in the most extreme case of the transition to the $T = 1$ (14·4 MeV) state, the RD central predicted cross section magnitude is comparable with the data and peaks at a scattering angle of 50° instead of the experimentally observed 35°, and the HJ central prediction, although an order of magnitude smaller than the RD, predicts a two-peaked structure not exhibited by the data.

Whilst in the other analyses reported in this paper we have seen different cross section magnitude predictions from the three different central forms, the higher multipole study of Fig. 5 is the only time that distinctly different cross sectional structure has been predicted, an observation which suggests that analyses of transitions to high spin states of *natural* parity may be instructive. Such transitions, which should be promoted largely by the central interaction components and should involve both proton and neutron transitions, may allow a definitive test of the different cross section structures predicted by the three forms defined here. Unfortunately, because the currently available spectroscopic descriptions of such states would probably also require that reaction analyses involve a significant core polarization amplitude which would severely reduce the sensitivity of the reaction as a test of effective interactions, such analyses must await more refined spectroscopic models.

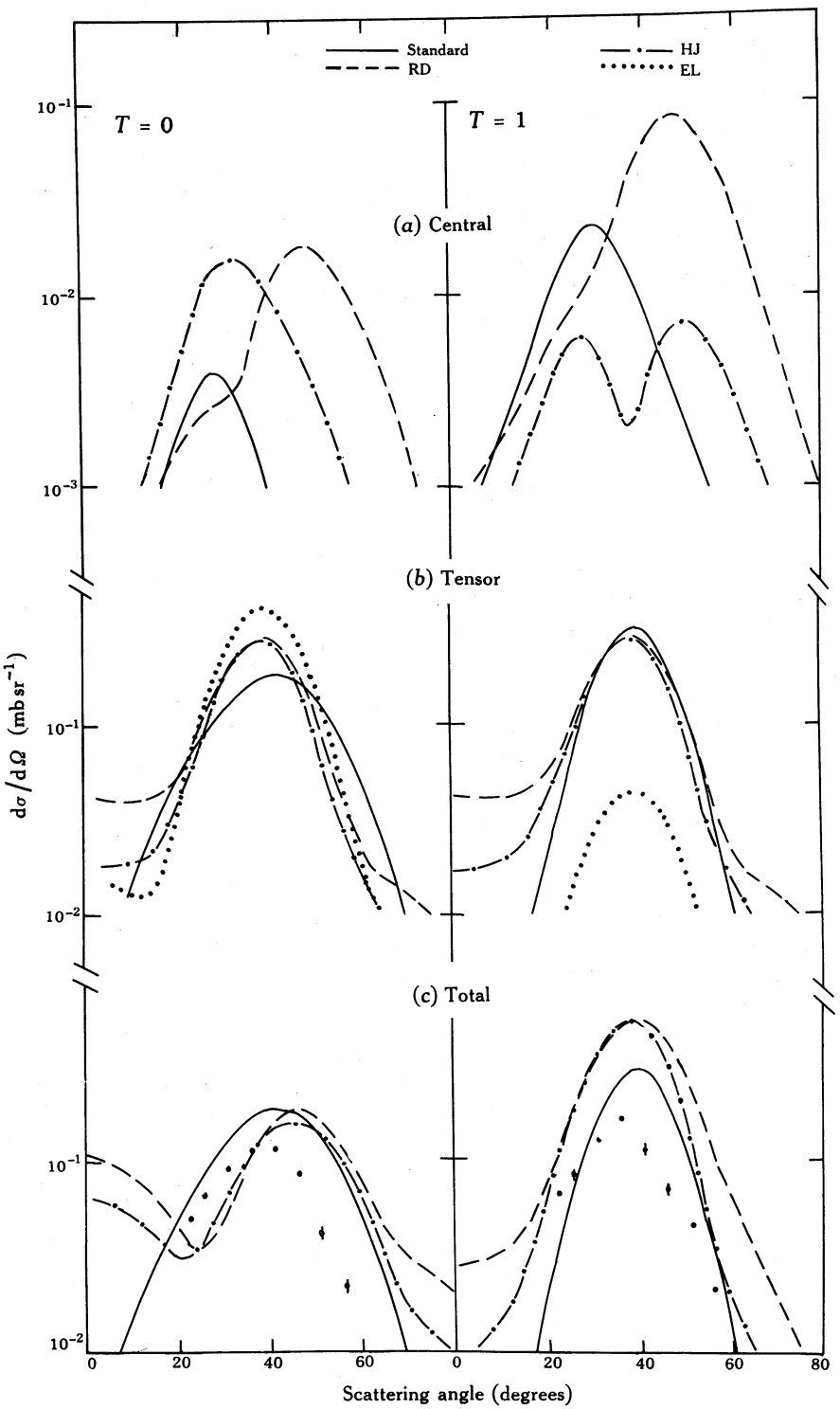

Fig. 5. Comparison of central, tensor and total force effective interaction results from DWA analyses of the inelastic scattering of 135 MeV protons exciting the isoscalar and isovector ($T = 0, 1$) 6^- states in ^{28}Si.

The total predictions shown in Fig. 5*c* all reflect the structure predicted by the tensor components. Each form produces a general cross section structure that is consistent with the experimentally observed one but all overestimate the magnitude. The Standard form, however, is superior, particularly for the excitation of the $T = 1$ (14·4 MeV) state, in which it overestimates the peak cross section by a factor of 2 compared with a factor of approximately 3 by the RD and HJ forms. Also, for the transition to the $T = 0$ (11·6 MeV) state, the Standard form predicts the peak cross section magnitude at 40°, in agreement with the data and in contrast to the 48° peak of the RD and HJ forms.

5. Conclusions

The effective interactions derived from 'realistic' potentials and the extensively used semi-phenomenological effective interaction have been subjected to a number of comparisons and have been applied to distorted wave analyses of a variety of transitions chosen to highlight different parts of the forces. Few significant differences between the forms have been observed, a result which supports the large body of work that has employed the semi-phenomenological (Standard) effective interaction in nucleon scattering analyses, and makes more credible the information (spectroscopy, effective charges, $B(EL)$ values and giant resonance details) extracted from those analyses.

The significant differences in the forms, seen clearly only in the high momentum components of the central force and high (J_4) moments of the interactions, are not as clearly distinguished in distorted wave analyses. Indeed all three forms examined produce comparable results for the distorted wave analyses of data in the ^{90}Zr region, when the reaction proceeds dominantly or exclusively via the two-body triplet isospin components. For analyses sensitive to both isoscalar and isovector two-body channels there seems to be a preference for the Standard form above those derived from the Reid and Hamada–Johnston potentials, a preference based on both agreement with cross section magnitude and some observed differences in predicted structure.

References

Adams, G. S., *et al.* (1977). *Phys. Rev. Lett.* **38**, 1387.
Amos, K., Faessler, A., Morrison, I., Smith, R., and Müther, H. (1978). *Nucl. Phys.* A **304**, 191.
Bechetti, F. D., and Greenlees, G. W. (1969). *Phys. Rev.* **182**, 1190.
Benenson, W., Austin, S. M., Paddock, R. A., and Love, W. G. (1968). *Phys. Rev.* **176**, 1268.
Bertsch, G., Borysowicz, J., McManus, H., and Love, W. G. (1977). *Nucl. Phys.* A **284**, 399.
Borysowicz, J., McManus, H., and Bertsch, G. (1977). Michigan State Univ. Internal Report.
Doering, R. R., Patterson, D. M., and Galonsky, A. (1975). *Phys. Rev.* C **12**, 378.
Eikemeier, H., and Hackenbroich, H. H. (1971). *Nucl. Phys.* A **169**, 407.
Elliott, J. P., Jackson, A. D., Mavromatis, H. A., Sanderson, E. A., and Singh, B. (1968). *Nucl. Phys.* A **121**, 241.
Fulmer, C. B., Ball, J. B., Scott, A., and Whiten, M. L. (1969). *Phys. Rev.* **181**, 1565.
Geramb, H. V. (1972). *Nucl. Phys.* A **183**, 582.
Geramb, H. V., and Amos, K. A. (1971). *Nucl. Phys.* A **163**, 337.
Geramb, H. V., *et al.* (1975). *Phys. Rev.* C **12**, 1967.
Hamada, T., and Johnston, I. D. (1962). *Nucl. Phys.* **34**, 382.
Horowitz, Y. S. (1972). *Nucl. Phys.* A **193**, 438.
Kennedy, D. L., Bolotin, H. H., Morrison, I., and Amos, K. (1978). *Nucl. Phys.* A **308**, 14.
Lebrun, D., *et al.* (1976). *Nucl. Phys.* A **265**, 291.

Love, W. G., Owen, L. W., Drisko, R. M., Stafford, R., and Philpott, R. J. (1969). *Phys. Lett.* B **29**, 478.
Love, W. G., and Satchler, G. R. (1970). *Nucl. Phys.* A **159**, 1.
Love, W. G., and Satchler, G. R. (1971). *Nucl. Phys.* A **172**, 449.
Morrison, I., Smith, R., and Amos, K. (1977). *J. Phys.* G **3**, 1689.
Nesci, P., and Amos, K. (1977). *Nucl. Phys.* A **284**, 239.
Reid, R. (1968). *Ann. Phys.* (*New York*) **50**, 411.
Rikus, L., Smith, R., Morrison, I., and Amos, K. (1977). *Nucl. Phys.* A **286**, 494.
Satchler, G. R. (1973). *Z. Phys.* **260**, 209.
Scott, A., Whiten, M. L., and Love, W. G. (1969). *Nucl. Phys.* A **137**, 445.
Smith, R. (1976). Ph.D. Thesis, Melbourne University.
Smith, R., Morton, J., Morrison, I., and Amos, K. (1978). *Aust. J. Phys.* **31**, 1.
Vergados, J. D., and Kuo, T. S. S. (1971). *Nucl. Phys.* A **168**, 225.
Willis, A., Geoffrion, B., Marty, N., Morlet, M., Rolland, C., and Tatischeff, B. (1968). *Nucl. Phys.* A **112**, 417.
Wong, C. W., and Wong, C. Y. (1967). *Nucl. Phys.* A **91**, 433.

Manuscript received 23 August 1978